Loss of coherency at interphase α/β boundary in Ti-6Al-4V alloys during deformation at 800°C

M. Cabibbo, A. Di Salvia, S. Zherebtsov

Ti-6Al-4V is one of the major titanium-based alloy especially for creep purposes. The alloy is generally subjected to high temperature deformation and it is generally used at warm/high temperatures. The alloy (α+β→β)-transus temperature is 995°C, that is, for temperatures within 995°C a mixed α+β phases microstructure characterizes the alloy mechanical behavior. The mutual relationship between the two phases, α_{HCP} and β_{BBC}, is such to have: $\{0001\}_\alpha$ || $\{110\}_\beta$; $\{11\text{-}20\}_\alpha$ || $\{111\}_\beta$, which in literature are known as Burgers orientation relationship. The coherency of the two phases is controlled by this crystallographic mutual relationship. Phases semi-coherency and non-coherency come from a non parallelism between the two boundary crystallographic planes. The present work focuses on the microstructure evolution of the α_{HCP}/β_{BBC} interface coherency character with hot compression at 800°C and a strain rate of $10^{-3}s^{-1}$ to an average true strain of ε = 0.29 and 0.69. Loss of coherency was determined to occur at a strain ε = 0.40. The present study was carried out by TEM inspections and SAEDP analyses.

Keywords:
Titanium alloys; Ti-6Al-4V; hot deformation; alpha-beta interphase; TEM

INTRODUCTION

One of the key microstructure features of titanium alloys is its polymorphism, that is a close-packed hexagonal lattice (α phase), which turns into a body-centered cubic lattice (β phase) above 882°C. β-stabilizer elements, such Mo, V, Cr, Fe, extend the area of the β existence down to room temperature, originating a vast class of engineering such dual phase titanium alloys. The most typical and commonly used two-phase titanium structure consists of lamellae of α phase slicing the β matrix. This structure can be easily induced by cooling from the single β phase area of the phase diagram. The α lamellae are likely to form either a number of colonies within the former β grains, or form a so-called basket-weave structure (Widmastatten). Formation of α phase from β during cooling meets the requirement of minimum energy through a specific orientation relationship (OR) between the two phases, which generated on cooling. The mutual relationship between the two crystallographic structures, α_{HCP} and β_{BBC}, was first proposed by Burgers (and since then known as the Burgers OR, [1,2]), and is as follows: $\{0001\}_\alpha$ || $\{110\}_\beta$; $\{11\text{-}20\}_\alpha$ || $\{111\}_\beta$. The occurrence of this OR can be considered as a precondition for the formation of a semi-coherent interphase boundary, which can be virtually transparent to dislocation sliding. For instance in [3] Ambard et al. showed a minimal structure element at low strain, being a colony of α lamellae and not a single α lamella.
Since a lamellar microstructure does not always ensure the mechanical and/or technological requirements, the need for producing a titanium alloy with a phase globular morphology can arise. Two-phase lamellar microstructure in titanium alloys does not transform into globular-shaped structure during a simple annealing treatment (in contrast to what happen to pearlite in steels), therefore straining up to ε ≈ 2-2.5, in the two-phase α/β area is required to form a homogeneous globular microstructure [4]. Indeed, during deformation α/β interface induces the microstructure evolution to sheroidize.
To date, very little data have been published on the OR modifications during deformation, especially at high temperatures [4-6]. Thus, the aim of the present work was to evaluate deviations from the α/β Burgers OR, during deformation at 800°C of a Ti-6Al-4V alloy.

M. Cabibbo*, A. Di Salvia
Dipartimento di Ingegneria Industriale e Scienze Matematiche (DIISM), Università Politecnica delle Marche, 60131 Ancona, Italia
*Email: m.cabibbo@univpm.it

S. Zherebtsov
Laboratory of bulk Nanostructured Materials
Belgorod State University,
85 Pobeda str., Belgorod, 308015 - Russia

MATERIAL, EXPERIMENTAL PROCEDURES AND METHOD

Material

The Ti-6Al-4V dual phase alloy used in this study have a chemical composition consisting of (wt.%): 6.3 Al, 4.1 V, 0.18 Fe, 0.03 Si, 0.02 Zr, 0.01 C, 0.018 O, 0.01 N, Ti bal.. The alloy was received in form of hot-rolled 16-mm diameter bars with a -transus (α+β→β) temperature of 995°C. To produce a stable microstructure consisting of α-lamellae colony embedded in the β-matrix, sections of the bars were subjected to a heat treatment of: heating at 995°C, soaking time of 15 min, then heating to 1010°C, soaking for 15 min, and furnace cooling to 800°C. Specimens were then soaked 20 min at 800°C and finally water quenched. The measured fraction of the β phase at the end of the heat treatment was $f_V(\beta) = 0.24 \pm 0.02$.

Experimental procedures

Hot compression tests were carried out in 12-mm cylindrical specimens of 8-mm in diameter. Specimens were isothermally pressed in air at 800°C in a Schenk® mechanical testing machine at a nominal strain rate of $10^{-3}s^{-1}$ and to an average true strain of ε = 0.29, and 0.69, corresponding to 25, and 50 pct. of height reduction, respectively. To preserve the deformed micro-

structure, specimens were water quenched right after the end of the hot deformation.
All the microstructure inspections were carried out using a transmission electron microscope (TEM). TEM discs were mechanically polished to flatness and then dimpled to a thickness of 30 μm before using a twin ion-miller (PIPS Gatan®) at an incidence angle of 4° in a cooled specimen stage. The microstructure inspections were carried out along the axial and deformation direction. A Philips CM20 transmission electron microscope (TEM) was used for all the microstructure analysis. The microscope is equipped with a double-tilt specimen holder (70 deg. excursion) and a cooling specimen stage; inspections were performed at 200kV.

Method
To obtain a statistical meaningful evaluation of the interphase boundary angles, three different TEM discs and a minimum of 5 different regions per disc, have been observed. At least 10 misorientation measurements across the α/β (0001)//(100) facet were carried out in every chosen material region. SAEDP was used for the calculation of the misorientation angles. TEM discs were tilted to show the $(0001)_\alpha$ // $(100)_\beta$ crystallographic relationship. Angles between the hexagonal α phase and cubic β phase were determined using a matrix conversion for reducing the 4-index hexagonal reciprocal lattice into a three-index notation. The corresponding misorientation angle was thus calculated using a rotational matrix. A schematic description of this crystallographic representative transformation is described hereafter:
The 4-index hexagonal zone axis: (u_e, v_e, t_e, w_e) reduces to $(u'_e = (u_e - t_e)/3, v'_e = (v_e - te_e)/3, w'_e = w_e/3)$,
the corresponding matrix conversion from hexagonal 4-index to 3-index is:

$$\begin{pmatrix} 1 & 1/2 & 0 \\ 0 & \sqrt{3}/2 & 0 \\ 0 & 0 & 1 \end{pmatrix}$$

which gives a zone axis of the hexagonal α phase of:

$$\begin{pmatrix} 1 & 1/2 & 0 \\ 0 & \sqrt{3}/2 & 0 \\ 0 & 0 & 1 \end{pmatrix} \begin{pmatrix} u_e \\ v_e \\ w_e \end{pmatrix} \left(a_e/a_c \quad a_e/a_c \quad c_e/a_c \right) =$$

Z.A.$_\alpha$ ($u'_{e\,ZA}$, $v'_{e\,ZA}$, $w'_{e\,ZA}$), and a zone axis of the cubic β phase = Z.A.$_\beta$ (p_{ZA}, q_{ZA}, r_{ZA}).
The misorientation angle, θ, is thus: $\theta = \arccos((p_{ZA}*a_c*u'_{e\,ZA}, + q_{ZA}*a_c*v'_{e\,ZA} + r_{ZA}*a_c*w'_{e\,ZA}) / (a_c*p_{ZA}^2 + a_c*q_{ZA}^2 + a_c*r_{ZA}^2)^{1/2} (a_c*u'^2_{e\,ZA} + a_c*v'^2_{e\,ZA} + a_c*w'^2_{e\,ZA})^{1/2}) 180/\pi$.
To quantify the deviation from the Burgers OR, two different methods were followed. Both methods are actually based on the determination of the existing angle of deviation between the $(0001)_\alpha$ // $(100)_\beta$ crystallographic relationship. The first method is based on the direct determination of the normal vector to the reflecting plane (according to [7]). The procedure consists of obtaining at least two diffraction spots belonging to two different crystallographic planes and lying in different goniometric angles. The simplest possible reflections correspond to a brightness maxima in dark-field (DF) mode. Thereafter, a orientation matrix describing every highlighted crystal orientation is generated. The associated experimental error of this method was within 2° of misorientation. The method could be successfully applied to defect-free phase. The second method is based on recording of selected area electron-diffraction patterns (SAEDP) for determining the angle between the $(0001)_\alpha$ // $(100)_\beta$ crystallographic OR. In this case, for each measurement, the disc was tilted to show the $(0001)_\alpha$ // $(100)_\beta$ and the angular deviation to this crystallographic OR was recorded and then used as input values for the rotational matrix using the formulation reported above. The associated experimental error of this second method was within 1° of misorientation.

RESULTS AND DISCUSSION

Undeformed Microstructure
The microstructure of the heat treated and water quenched alloy consisted of lamellar α-colonies within prior β grains (Fig. 1 a). Mean α lamellae thickness was of 1.8 μm. TEM inspections of the undeformed alloy showed quite few dislocations and fewer dislocation walls within the α phase. The β phase microstructure is decorated by martensitic α' phase particles (Fig. 1b). The structure contrast showed at the α/β interphase indicates the presence of tangled dislocation and a high level of internal stress (Fig. 1 b and c). In particular, Fig. 1c showed a relaxation phenomenon within the α phase in the next vicinity of the α/β interface. The higher internal stress and strength of the β phase is therefore attribute to the diffuse presence of the α' particle strengthening. On the other hand, the phase lattice distortion near the α/β interface boundaries and the observed tangled dislocations within the interphase can hardly be associated with a coherent boundary. The presence of Moiré fringes in some region of the interphase length are indeed associated to a partial crystallographic matching, thereby implying at least a semi-coherent character of the α/β interfaces.

Microstructure of the Ti-6Al-4V alloy compressed at 800°C
During compression at 800°C/ε=0.29, the alloy microstructure developed a evident phase modification. β grains elongated considerably, and α lamellae rotated toward the metal flow direction. Localized lamellae bending and shearing frequently led to fragmentation of the α phase (Fig. 2). The dislocation density within the α phase considerably raised compared to the undeformed condition. Moreover, irregularly shaped sub-grains and curved boundaries start to develop in the α phase. On the contrary, the β phase was characterized by a diffuse presence of loose arrays of dislocations.

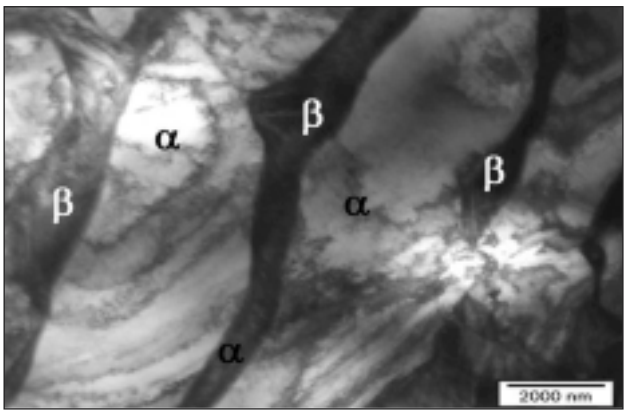

FIG. 2 ***BF-TEM image showing the microstructure of the Ti-6Al-4V alloy compressed at 800°C/ε=0.29. Gliding dislocations lie in a different crystallographic plane and therefore are not visible here.***
Immagine in campo chiaro della microstruttura della lega Ti-6Al-4V dopo compressione a 800°C/ε=0.29. Le dislocazioni di scorrimento giacciono su un differente piano cristallografico e non sono pertanto visibili in queste micrografie.

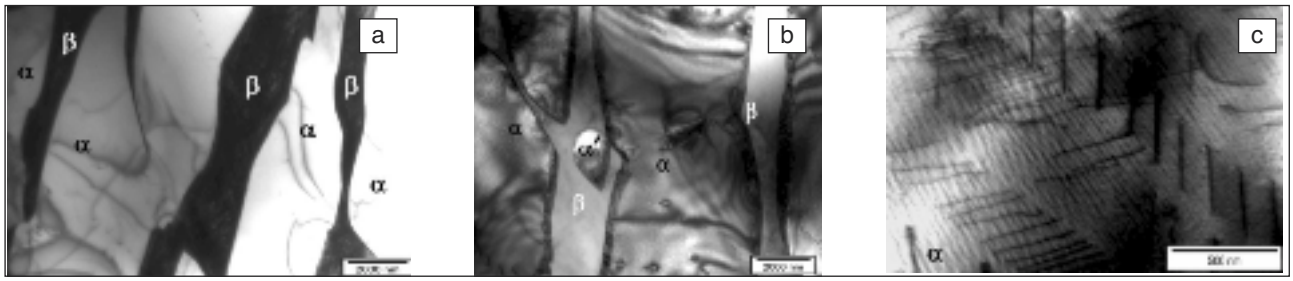

FIG. 1 ***(a) and (b) Two different magnified BF-TEM images showing three different regions of the initial undeformed microstructure of the Ti-6Al-4V (alloy heat treated 15min/995°C, heated to 15min/1010°C, furnace cooled to 800°C, maintained 20 min, and finally water quenched). (b) an example of α' martensite grain in the β plate-like phase; (c) a detail of the α/β interface boundary showing forest of tangled dislocations.***

(a) e (b) Immagini TEM a due diversi ingrandimenti e tre diverse zone della lega non-deformata (lega sottoposta a trattamento termico di 15min/995°C, seguita a riscaldamento di 15min/1010°C, raffreddamento in forno a 800°C, mantenimento per 20 min, e spegnimento in acqua). (b) Un esempio di grano martensitico α' all'interno della fase β;(c) dettaglio del bordo di interfase α/β che mostra la foresta di dislocazioni.

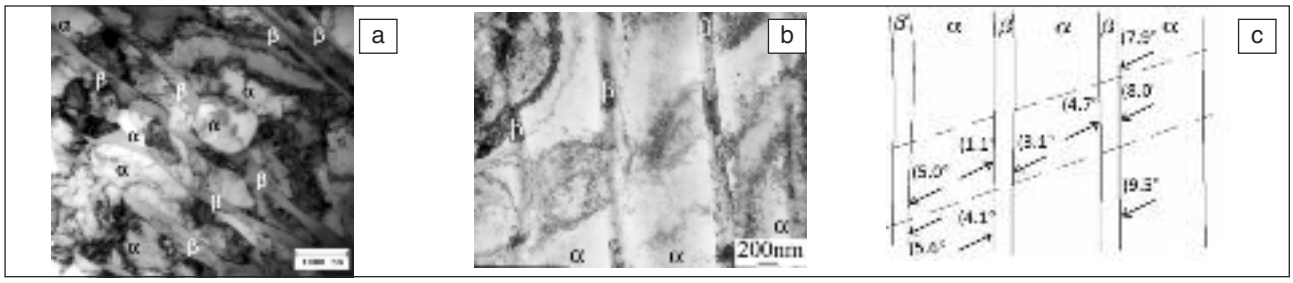

FIG. 3 ***(a) and (b) BF-TEM image of the Ti-6Al-4V alloy microstructure compressed at 800°C/ε=0.69; (c) schematic representation of the α/β boundaries showing the SAEDP measured angles between normal lines to the planes*** $(0001)_{\alpha}^{HCP}$ ***and*** $(110)_{\beta}^{BCC}$***.***

(a) e (b) Immagine in campo chiaro della microstruttura della lega Ti-6Al-4V dopo compressione a 800°C/e=0.69; (c) rappresentazione schematica dei bordi a/b con i relative angoli di disorientazione tra le normali ai piani $(0001)_{\alpha}^{HCP}$ *and* $(110)_{\beta}^{BCC}$ *determinati mediante SAEDP.*

At the strain of ε=0.69, the alloy microstructure changed significantly (Fig. 3). Although the α lamellae were still aligned toward the plastic deformation metal flow, the vast majority of the lamellae contained either low and high angle boundaries (Fig. 3). The β phase appeared as long ribbon-like laths; interface boundaries are mainly straight and sharp, without any significant sign of stress between the two adjacent phases, which could indicate a loss of coherency between the two phases (Fig. 3a). Yet, in some cases, boundaries showed a fringe contrast parallel to the lath extension, thus revealing a perfect crystallographic matching to the surrounding α phase (Fig. 3b and c).

Burgers or evolution with deformation straining at 800°C

In the general case, a coherent interphase boundary is defined as a boundary between two phases where planes of one phase turn into planes of other phase without any gaps. Conjugation of the lattices of two phases (supposing that interatomic spacing of those phases is always different) may be accommodated by means of elastic deformation. Increase in the mismatch between the phase lattices obviously rises energy of the interphase boundary and, beginning from a certain stage, compensation in lattice mismatch becomes more energetically favorable through introduction of misfit dislocations. The boundary still remains coherent in the spaces between misfit dislocations. Therefore, if the inter-dislocation spaces are big enough the boundary can be considered as a semi-coherent one. As the distance of the misfit dislocations reduces the level of coherency decreases and boundary energy rises accordingly. So energy of interphase boundary can be considered as a criteria of coherency: higher energy corresponds to lower coherency of the boundary.

The energy of the boundary can be evaluated quantitatively by means of the semi-coherent boundary model proposed by Liebmann [8-10]. In this model mismatches in an interphase boundary can be accommodated by two mutually perpendicular arrays of edge dislocations which lie in the plane of the boundary. Thus, the energy, E_i, of the interphase boundary can be expresses through the sum of energies of elastic strain of separate dislocations (Eq. (1)):

$$E_i = C\{[|L_2\, L_1|/\ln(L_1||L_2 - L_1|) + |B_2 - B_1|\ln(B_1/|B_2 - B_1|)] \quad (1)$$

where $C = G/[4\pi(1-\nu)]$, G is the shear modulus, ν the Poisson ratio, L_1 and L_2 the interatomic spacing in both phases in a direction parallel to the phase growth direction, B_1 and B_2 are the phase interatomic spacing in the transversal direction.

Based on the data published by Furukawa et al.[11] for titanium alloys, α and β phases conjugate through the following crystallographic planes (see scheme of Fig. 4 a and b): along the side face of the β-plate $(0001)_{\alpha}$ || $(110)_{\beta}$, and along the broad face of the β-plate $(11\text{-}15\text{-}40)_{\alpha}$ || $(11\text{-}11\ 13)_{\beta}$. Moreover, according to [9,10] this crystallographic relationship decomposes into two conjugating relationships corresponding to the actual facets boundary morphology generates along the α/β interface, as shown in Fig. 4. The facets are perpendicular to each other, with

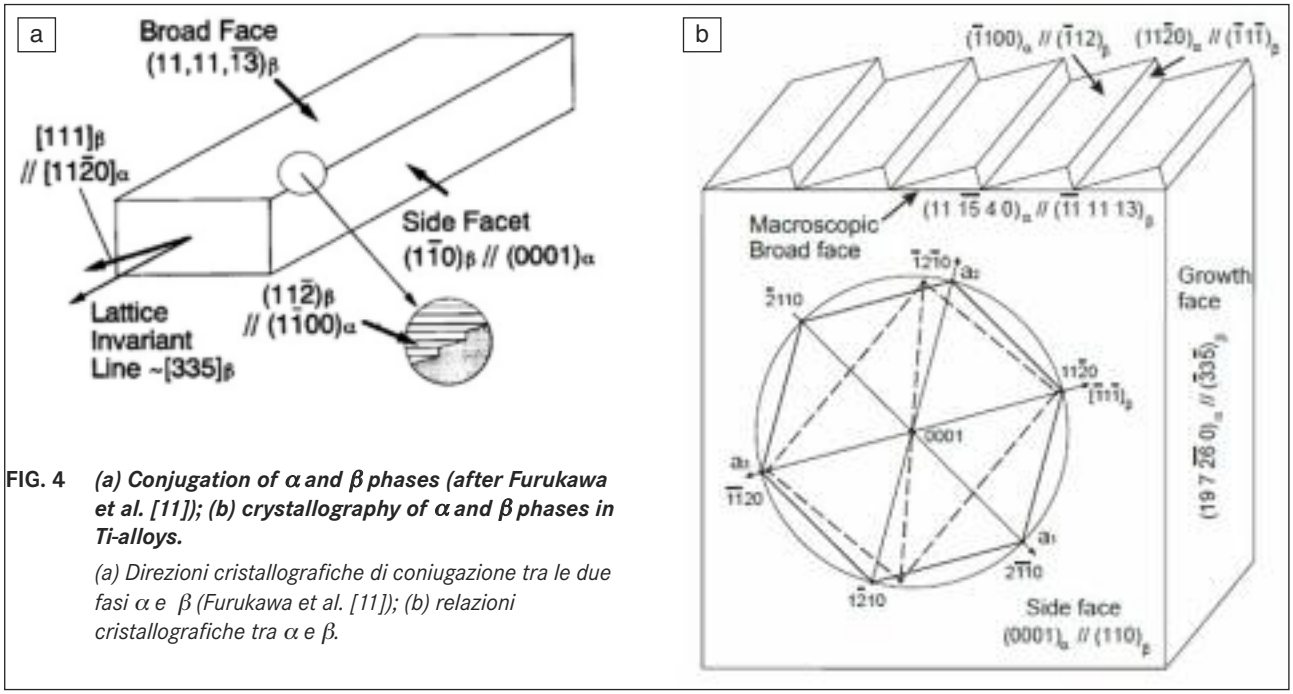

FIG. 4 ***(a) Conjugation of α and β phases (after Furukawa et al. [11]); (b) crystallography of α and β phases in Ti-alloys.***

(a) Direzioni cristallografiche di coniugazione tra le due fasi α e β (Furukawa et al. [11]); (b) relazioni cristallografiche tra α e β.

Plane of conjugation (Macro)	Plane of conjugation (Facets)	Longitudinal direction	Interatomic spacing in the longitudinal direction, nm		Transverse direction	Interatomic spacing in the trasversal direction, nm		Energy of interphase boundary
			L_α	L_β		B_α	B_β	
$(0001)_\alpha$ // $(110)_\beta$		$[-3\ 3\ -5]_\beta$ // $[15\ 11\ -25\ 0]_\alpha$	0,2952	0,325	$[11\ -11\ 13]_\beta$ // $[7\ -19\ 12\ 0]_\alpha$	0.5112	0,4639	**0,188** C = 0.641
$(11\ -15\ 4\ 0)_\alpha$ // $(11\ -11\ 13)_\beta$		$[-3\ 3\ -5]_\beta$ // $[15\ 11\ -26\ 0]_\alpha$	3,9711	9,3948	$[110]_\beta$ // $[0001]_\alpha$	0,4679	0,4639	**2,998** C = 10,23
	$(-100)_\alpha$ // $(-112)_\beta$	$[-111]_\beta$ // $[11-20]_\alpha$	0,2952	0,7334	$[110]_\beta$ // $[0001]_\alpha$	0.4679	0,4639	**0,245** C = 0.835
	$(11-20)_\alpha$ // $(-111)_\beta$	$[-111]_\beta$ // $[11-20]_\alpha$	0,5113	0,8034	$[110]_\beta$ // $[0001]_\alpha$	0.4679	0,4639	**0,315** C = 1.073
$(19\ 7\ -25\ 0)_\alpha$ // $(-33-5)_\beta$		$[11\ -11\ 13]_\beta$ // $[7\ -19\ 12\ 0]_\alpha$	5.878	1,9126	$[110]_\beta$ // $[0001]_\alpha$	0.4679	0,4639	**1,637** C = 5.562
C = G/[4π(1 - ν)]								

TAB. 1 ***Data for the calculation of α/β interphase boundary energies according to Eq. (1).***

Dati relative al calcolo delle energie di bordo di interfase α/β mediante l'Eq. (1).

an horizontal deviation of 14,4°: and $(-1\ 1\ 0\ 0)_\alpha$ || $(-1\ 1\ 2)_\beta$ and $(1\ 1\text{-}2\ 0)_\alpha$ || $(-1\ 1\text{-}1)_\beta$, with a growing face of the β-plate with a more complex crystallographic OR: $(19\ 7\ -26\ 0)_\alpha$ || $(-3\ 3\ -5)_\beta$. Table 1 reports data of Eq. (1) and the obtained values of interphase boundary energies. Data in Table 1 show that the lowest energy (0,188 , where C = G/[4π(1-ν)] has the conjugation boundary of planes $(0001)_\alpha$ and $(110)_\beta$. On the other hand, the broader surface, which is conjugated by OR $(1\ 1\ -2\ 0)_\alpha$ || $(-1\ 1\ -1)_\beta$ and $(-1\ 1\ 0\ 0)_\alpha$ || $(-1\ 1\ 2)_\beta$ have higher energy (0,245 and 0,315, respectively).

Van der Merwe, in [12], and Read and Shockley, in [13], showed that when the crystal structures between the matrix and its second phase are different to a significant extent, displacement of both fully and partially coherent boundaries in the normal direction is impossible by a diffusion mechanism. This was motivated by the fact that it would require substitutional atoms to temporarily locate in interstitial sites and thus inducing the matrix/second phase interface to a fully coherency, but this would means that a new and different crystallographic structure is generated. Hence these boundaries must migrate by a dislocation ledge mechanism. According to the ledge mechanism model [13], the terraces of the ledges are partially or fully coherent, while inter-terrace steps have a disordered structure.

In the present case, data of Table 1 show that the boundary normal to the growth direction has a rather high energy and hence this boundary is non-coherent (although it is energetically possible for the boundary plane $(19\ 7\ -26\ 0)_\alpha$ || $(-3\ 3\ -5)_\beta$ to split into facets with lower energy).

Concerning the evolution of the initially semi-coherent interphase boundary during deformation, a number of investigations (e.g. [14]) showed the semi-coherent α/β boundary to be crossed by sliding dislocations, thus making the α+β colony behave like

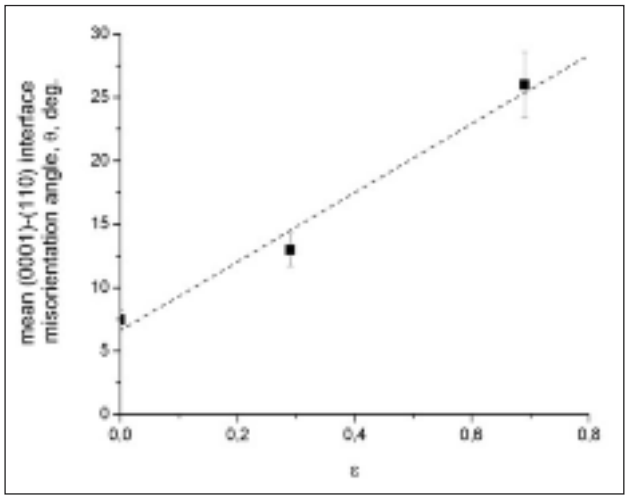

FIG. 5
Mean misorientation angles (deg.) between the crystallographic planes $(0001)_\alpha$ and $(110)_\beta$ vs. strain. The data linear interpolation K slope, by expressing angles in radiant, is 0.33.

Disorientazione angolare media (in gradi) tra i piani cristallografici $(0001)_\alpha$ and $(110)_\beta$ in funzione della deformazione plastica imposta. La pendenza, K, dell'interpolazione lineare dei dati sperimentali vale 0.33, previa conversione dei valori angolari in radianti.

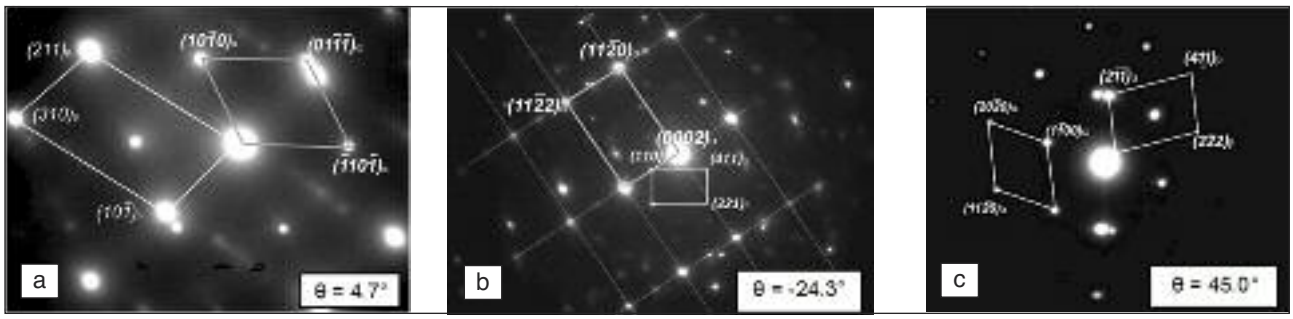

FIG. 6 ***(a) SAEDP across the α/β interface in the undeformed Ti-6Al-4V alloys, (b) in the alloy compressed at 800°C/ε=0.29, and (c) at 800°C/ε=0.69. Corresponding interface misorientation angles are reported at the bottom of the corresponding SAEDP.***

(a) Esempio di SAEDP ottenute in corrispondenza delle interfasi α/β nella lega non-deformata, (b) nelle due condizioni di compressione a 800°C/ε=0.29 e (c) a 800°C/ε=0.69. Gli angoli di disorientazione così determinati sono indicati nella parte basse di ogni SAEDP.

a grain, at least in the early stage of deformation. However, during deformation, the energy of interphase boundary increases (and simultaneously coherency deteriorates) due to interaction between boundaries and dislocations. In fact, the α-plate broad face (in the macroscopic scale formed by planes of $(11\text{-}15\text{-}4\ 0)_\alpha$ || $(11\text{-}11\ 13)_\beta$) has the largest boundary surface and, consequently, it greatly influences the interphase boundary evolution with deformation. Any change of interphase boundaries during deformation is associated with formation of dislocation arrays along the boundary plane, resulting in loss of coherency along that specific crystallographic plane.

Deviation from the Burgers OR at the α/β interface was quantitatively evaluated measuring the existing angle between the normal vectors to the crystallographic planes $(0001)_\alpha$ and $(110)_\beta$, which, for fully coherent interfaces, according to the Burgers OR, must be parallel. The obtained data were plotted as a function of strain and showed in Fig. 5. An example of the use of SAEDP for the interface angle determination is shown in Fig. 6. The noticeable deviation from the Burgers OR in the undeformed alloys (mean value of 7.5 deg.) may be associated to some non-equilibrium state of the microstructure. Actually, the water quenching have induced a metastable state of the β matrix and formation of martensite phases within β, as shown in Fig. 1b. Both factors are responsible for the distortion of the β-lattice and thereafter for the interface angle deviation. In some other cases, slower cooling to same alloy from a lower temperature (600°C), and therefore from a single-phase β region, did not induce any significant deviation from the Burgers OR [15], as sown through the here reported pole figure (Fig. 7).

The interphase boundary energy increment at a small strain can be determined using a formula which describes the energy of a low-angle boundary in a single phase material. The grain boundary energy as a function of misorientation was first calculated by van der Merwe [12] and Read and Shockley [13], and it can be express as (Eq. (2):

$$E_d = (Gb\theta)/\{4\pi(1-\nu)(1-\ln(2\pi\theta))\} \quad (2)$$

where b is the Burgers vector, and θ is dislocation boundary misorientation.

The dislocation boundary misorientation can be expressed as a function of the strain through Eq. (3):

$$\theta = K\varepsilon \quad (3)$$

where ε is the strain to which the material is subjected, and K is a material dependent constant. Actually, the physical interpretation of K is associated with the rate of misorientation growth of dislocation boundaries during deformation. Combining Eqs. (1), (2) and (3), the interphase boundary energy can be expressed in terms of strain (Eq. (4)):

$$E = E_i + E_d = C\{[|L_\alpha - L_\beta|\ \ln(L_\alpha/|L_\alpha - L_\beta|) + |B_\alpha - B_\beta|\ \ln(B_\alpha/|B_\alpha - B_\beta|)] + [bK\varepsilon\ (1 - \ln(2\pi K\varepsilon))]\} \quad (4)$$

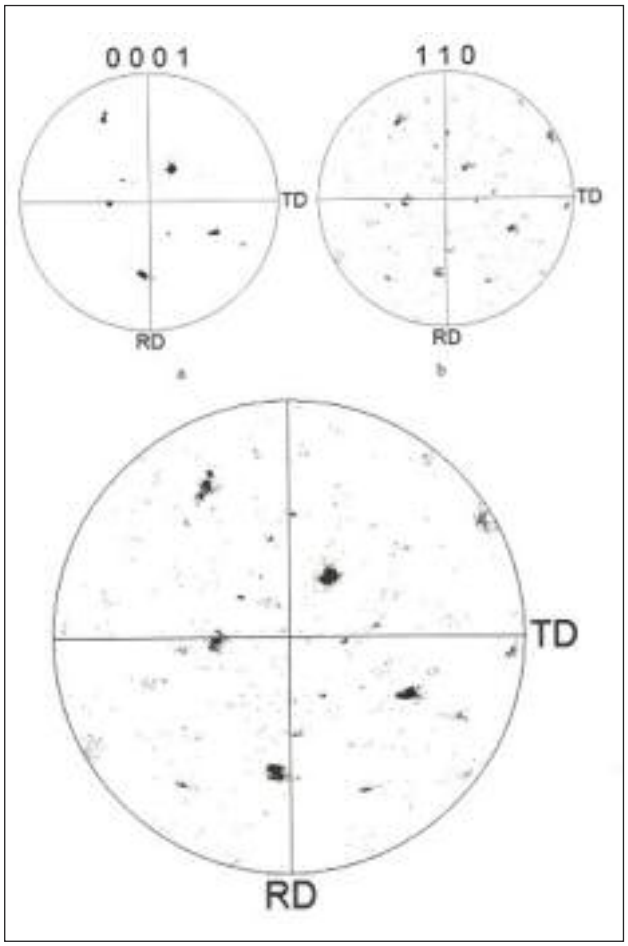

FIG. 7
Pole figure of (0001) (a) and (110) (b) of Ti-6Al-4V cooled in air from 600°C; overlapping of same two pole figures is shown beneath. No significant deviation from the Burgers OR occurred (after Mironov et al. [15]).

Figura polare dei piani (0001) (a) e (110) (b) di una lega Ti-6Al-4V raffreddata in aria da 600°C; la figura polare in basso mostra la sovrapposizione delle due figure polari. La sovrapposizione mostra chiaramente l'assenza di apprezzabili deviazioni dalle relazioni di orientazione di Burgers (figura riprodotta da un lavoro pubblicato da Mironov et al. [15]).

The value of E_i is reported in Table 1. The coefficient K can varies in a wide range. For cold deformation cupper [16,17] and stainless steel [18], the values of K were found ~0.1; in hot rolling stainless steel, a deformation temperature increment leads to an equivalent K increment up to 0.21 [17], and even to 0.7, during super-plastic deformation of aluminum alloy [19].
At the same time, the wall dislocation generation rate along already existing obstacles (as interphase boundaries) is higher than in a single-phase metal. Departure from Burgers OR, in the present case of the alloy compressed at 800°C/ε=0.29 (Fig. 2) yield K = 0.33. Same value of K was found at a strain ε=0.69. Therefore in the whole range of tested compression strain, the rate of α/β interface misorientation was constant (Fig. 5). In the undeformed condition, mean interface misorientation was 7.5 ± 0.5 deg., at ε=0.29, the mean misorientation, θ, raised to 13 ± 1 deg., and at ε=0.69 up to 26 ± 2 deg.. Mean misorientation angles for each region and all the three TEM-discs observed are reported in Table 2. The table shows that, at ε=0.29, at least half of the misorientation angle population of interface boundaries have a high-angle character, while, at ε=0.69, all misorientation are well above 15 deg.. Thence, interface was semi-coherent at the initial Ti-6Al-4V, water quenched undeformed condition, turning into non-coherent already after a strain of ε≥0.4 (θ>15 deg.). That is, the transition form semi-coherency to fully non-coherency occurred for a thickness reduction of 30-35%, which is in good agreement with other previously published studies [15,20,21].
Substituting the K value in Eq.(4), the dependency of interphase boundary energy was determined and plotted as a function of

Calculated $(0001)_\alpha^{HCP}$ and $(110)_\beta^{BCC}$ interface misorientation angle, θ, deg.																$<\|\theta\|>$, deg. each disc	$<\|\theta\|>$, deg. All discs
	$<\|\theta\|>$ per disc region (disc 1)					$<\|\theta\|>$ per disc region (disc 2)					$<\|\theta\|>$ per disc region (disc 3)						
undeformed	4.2	7.4	3.8	8.1	10.4	5.8	7.3	11.8	2.5	9.3	7.9	8.4	7.3	9.3	8.8	6.8 7.3 8.3	**7.5±0.5**
800°C / $\varepsilon = 0.29$	6.8	11.8	14.7	16.1	17.5	11.4	8.9	7.9	15.7	16.9	14.4	15.8	14.2	16.3	12.5	13.4 12.2 14.6	**13±1**
800°C / $\varepsilon = 0.69$	19.5	23.9	26.2	28.5	22.6	26.8	27.5	24.2	26.5	29.4	31.5	34.7	24.1	22.7	21.9	24.1 25.7 27	**26±1**

TAB. 2 ***Mean interface misorientation across the $(0001)_\alpha^{HCP}$ and $(110)_\beta^{BCC}$ interface planes; data refer to all the 5 different regions in each of the 3 TEM-discs inspected. Misorientation angle of the undeformed, and the two compressed conditions (800°C/ε=0.29 and ε=0.69) are included. Last column reports the mean misorientation values considering all the different TEM-disc regions.***

Disorientazione angolare media dei piani di interfase $(0001)_\alpha^{HCP}$ e $(110)_\beta^{BCC}$; i dati qui riportati si riferiscono a tutte e 5 le zone in ciascuno dei 3 dischetti TEM analizzati. Sono riportati i valori relativi alla lega non-deformata e alle due condizioni di compressione a caldo (800°C/ε=0.29 and ε=0.69). L'ultima colonna presenta i valori medi considerando tutte le zone di indagine.

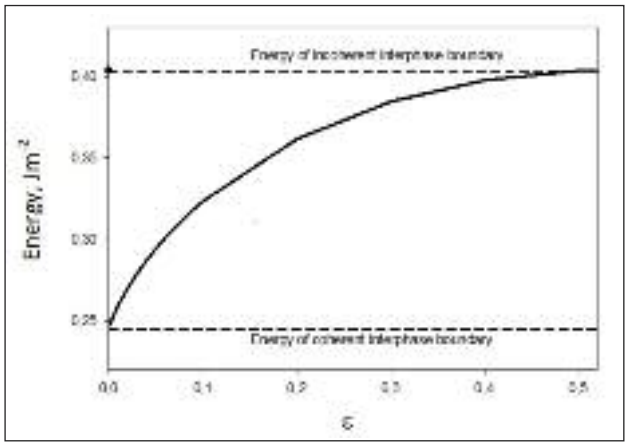

FIG. 8 ***Energy of interphase boundary (-1100)$_\alpha$ || (-112)$_\beta$ as a function of strain for Ti-6Al-4V alloy with a α and β lamellar microstructure.***

Energia di confine di interfase (-1100)$_\alpha$ || (-112)$_\beta$ in funzione della deformazione plastic della lega Ti-6Al-4V con struttura lamellare delle due fasi α e β.

strain (Fig. 8). It is seen, that the energy of interphase boundary changed quickly at the earlier stages of deformation reaching the maximum value at the strain ε≈ 0.5 (corresponding to ~40% of height reduction). This value, as shown in Fig. 8, can be considered a saturation limit and therefore, it is expected that further deformation will not induce any significant increment of the interface misorientation.

Loss of coherency is likely to hinder dislocation sliding across the non-coherent α/β interfaces, resulting in a process of differentiated deformation of each microstructure phase (namely, both α and β) which in fact accelerates the spheroidization morphology of the two phases. In some previous works ([22] to cite but one), acceleration of globularization of Ti-6Al-4V titanium alloy after deformation above 0.3 (corresponds to 25% of height reduction) was reported. This phenomenon was associated with loss of coherency of α/β interphase boundaries. The same assumption of coherency loss of interphase boundaries in Ti-6Al-4V alloy in the compression deformation range of 0.30-0.70 in at 600°C was made in [15], on the basis of EBSD analysis. Thus, results here obtained are fully consistent to previously published data.

SUMMARY

The α/β interface coherency of a Ti-6Al-4V alloy compressed at 800°C/10^{-3}s^{-1} and to an average true strain of ε = 0.29, and 0.69 was characterized. The deviations from the mutual Burgers OR: {0001}$_\alpha$ || {110}$_\beta$; {11-20}$_\alpha$ || {111}$_\beta$ were evaluated by TEM SAEDP analyses. It was found that coherency is lost at a strain ε = 0.40. At ε=0.29 interfaces were mostly semi-coherent and at least half of the misorientation angle population had a high-angle character. At ε=0.69, the interfaces were essentially non-coherent and all misorientation were found to be well above 15 deg. (high-angle interfaces). Interphase boundary energy changed quickly at the earlier stages of deformation reaching the maximum value at the strain ε ≈ 0.5 where a saturation limit was reached. Therefore, it is expected that further deformation will not induce any significant interface misorientation rise.

REFERENCES

[1] W.G. Burgers, Physica, Vol. 1 (1934) p.561.
[2] U. Dahmen. Acta Metall., Vol. 30 (1982), p.63.
[3] A. Ambard, L. Guetaz, F. Louchet, D. Guichard, Mater. Sci. Eng. A, Vol. 319-321 (2001) p.404.
[4] S.L. Semiatin, V. Seethsraman, I. Weiss. Mater. Sci. Eng. A, Vol. 263 (1999) pp.257-271.
[5] R. Ding, Z.X. Guo. Mater. Sci. Eng. A, Vol. 365 (2004) pp.172-179.
[6] L. Zeng, T.R. Bieler. Mater. Sci. Eng. A, Vol. 392 (2005) pp.403-414.
[7] R.Z. Valiev, A.N. Vergazov, V.Y. Gertsman. Nauka Pub., Moscow (1991), p.232.
[8] W.K. Liebmann and E.A. Miller. J. Appl. Phys., Vol. 34 (1963), p. 2653.
[9] D. Bhattacharyya, G. B. Viswanathan, R. Denkenberger, D. Furrer, Hamish L. Fraser. Acta Mater. Vol. 51 (2003), p. 4679.
[10] S. Suri, G. B. Viswanathan, T. Neeraj, D. -H. Hou, M. J. Mills. Acta Mater. Vol. 47 (1999), p. 1019.
[11] T. Furuhara, S. Takagi, H. Watanabe, T. Maki. Metall. Trans. A, Vol. 27 (1996), p. 1635.
[12] J.H. van der Merwe. Proc. Phys. Soc. A 63 (1950), pp. 616-637.
[13] W.T. Read, W. Shockle. Phys. Rev., Vol. 78 (3), (1950), pp. 275-289.
[14] Q. Liu, X. Huang, M. Yao and J. Yang, Acta Metall. Mater., Vol. 40, (1992) p. 1753.
[15] S. Mironov, M. Murzinova, S. Zherebtsov, G.A. Salishchev, S.L. Semiatin. Acta Mater., Vol. 57 (2009) p. 2470.
[16] A. Belyakov, W. Gao, H. Miura and T. Sakai. Metall. Mater. Trans. A, Vol. 29 (1998) p. 2957.
[17] A. Belyakov, T. Sakai, H. Miura and K. Tsuzaki. Phil. Mag. A, Vol. 81 (2001) p. 2629.
[18] A. Belyakov, Y. Kimura and K. Tsuzaki. Mater. Sci. Forum, Vols. 503-504 (2006) p. 323.
[19] K. Tsuzaki, X. Huang and T. Maki. Acta Mater., Vol. 44 (1996) p. 4491.
[20] R. Zherebstov, G. Salishchev, S.L. Semiatin. Phil. Mag. Lett., Vol. 90 (2002) p. 903.
[21] R. Zherebstov, S. Mironov, M. Murzinova, G. Salishchev, S.L. Semiatin. Mater. Sci. Forum, Vols. 584-586 (2008) p. 771.
[22] T. Furuhara, T. Ogawa, T. Maki. Phil. Mag. Lett., Vol. 72 (1995) p. 175.

Abstract

Perdita di coerenza dei confine di interfase α/β in una lega Ti-6Al-4V sottoposta a deformazione plastica a 800°C

Parole Chiave: Titanio e leghe, trasform. di fase, deformazioni plastiche, microscopia elettronica

La lega Ti-6Al-4V è una delle più importanti e diffuse leghe di titanio, soprattutto nel campo delle alte temperature tipiche di comportamento a creep. Infatti, tale lega è generalmente sottoposta a deformazioni ad elevata temperatura e a forti esposizioni ad alte temperature in esercizio. La lega ha una transizione di fase (α+β→β) a 995°C, pertanto, per temperature inferiori la microstruttura è caratterizzata dalla presenza delle due fasi α+β che pertanto ne influenzano i comportamenti meccanici. La relazione cristallografica esistente tra le due fasi, α_{HCP} e β_{BBC}, è del tipo: {0001}$_\alpha$ || {110}$_\beta$; {11-20}$_\alpha$ || {111}$_\beta$, tali relazioni sono note come orientazioni di Burgers. Lo stato di coerenza delle due fasi è legato al mantenimento di tali relazioni cristallografiche. La coerenza tra le fasi viene a mancare in favore di una semi-coerenza o non-coerenza ogni volta che il parallelismo tra i piani cri-

stallografici di Burgers viene perso. Il presente lavoro è dedicato allo studio evolutivo della microstrutturale in termini di stato di coerenza dell'interfaccia α_{HCP}/β_{BBC} di una lega Ti-6Al-4V compressa a 800°C ad una velocità di deformazione di $10^{-3}s^{-1}$ e fino a livelli deformativi di ε= 0.29 e 0.69. Perdita di coerenza dell'interfaccia tra le due fasi è stata accertata a partire da ε= 0.40. L'intero studio e caratterizzazione microstrutturale sono stati portati avanti mediante microscopia elettronica a trasmissione (TEM) e analisi delle SAEDP (Selected Area Electron Diffraction Patterns).
Le analisi hanno permesso di apprezzare le deviazioni cristallografiche dalla inter-relazione planare di Burgers ($\{0001\}_\alpha \parallel \{110\}_\beta$; $\{11\text{-}20\}_\alpha \parallel \{111\}_\beta$). Tale relazione garantisce la piena coerenza dell'interfase α/β ed ogni scostamento angolare da essa implica progressive perdita di coerenza all'interfase. Si è così potuto determinare il limite di deformazione plastica oltre il quale l'interfase perde la coerenza in favore di uno stato di non-coerenza attraverso progressivi passaggi a stati di semi-coerenza. Tale limite è di ε= 0.40. A ε= 0.29, le interface sono prevalentemente semi-coerenti ed almeno la metà delle disorientazioni angolari medie presentano valori angolari superiori ai 15 gradi, il che denota una popolazione di interfacce semi- e non-coerenti. A ε = 0.69, le interface sono quasi interamente non-coerenti, tutti I valori medi di disorientazione angolare sono superiori ai 15 gradi. L'energia dei bordi di interface aumenta considerevolmente nei primi stadi di deformazione, per poi raggiungere un limite di saturazione a $\varepsilon \approx 0.5$. Pertanto, è lecito aspettarsi che livelli di deformazione superiori a quelli raggiunti nel presente lavoro non siano in grado di incrementare ulteriormente la deviazione angolare media dei bordi di interfase, i quali peraltro avevano già perso lo stato di coerenza.